AXIAL COMPRESSION TEST AND PARAMETER ANALYSIS OF THIN-WALLED CONCRETE-FILLED STEEL TUBULAR COLUMNS WITHOUT AND WITH STIFFENERS

ZHENSHAN WANG[1,2]*, YONGJIAN FENG[1], JUNLONG LU[1], HONGCHAO GUO[1], JIANBO TIAN[1]
[1] *State Key Laboratory Base of Eco-Hydraulic Engineering in Arid Area, Xi'an University of Technology, Xi'an 710048, China;*
[2] *School of Civil and Architectural Engineering, Xi'an University of Technology, Xi'an 710048, China.*

An experimental investigation was conducted to study the axial compression behavior of thin-walled concrete-filled steel tubular (TWCFST) column with spiral stiffeners. In order to explore the impact of spiral stiffener on the engineering properties of TWCFST column, the columns without and with 3 types of stiffening form tests were carried out. The mechanical properties and failure mechanism of 4 types of columns were observed and analyzed, and the stress-strain curves and load-displacement curves were obtained. Test results showed that, compared with the ordinary TWCFST column, the TWCFST column with spiral stiffeners could effectively improve the bearing capacity. Meanwhile, the spiral stiffener could effectively combine with the internal concrete, which would improve the stability of the steel pipe wall, delay the local buckling, and limit the penetration cracks caused by the internal filling concrete. The spiral ribbed concrete column had better integrity and significantly improved deformation capacity. Based on the experimental research, the parameters of the diameter-thickness ratio of the round steel tube, the width-thickness ratio of the spiral stiffener and the pitch were analyzed, and the design suggestions were put forward. This paper proposed a new type of restrained steel tubular concrete member. The research results would provide some technical support for the engineering application of the composite column.

Keywords: *concrete-filled steel tubular column; stiffener pipe; axial compression test; failure mode; finite element simulation*

1. Introduction

The use of thin-walled concrete-filled steel tubular columns has been increasingly developed in structural engineering, due to their high bearing capacity, good deformability and high degree of industrialization. Various analytical and experimental studies have been conducted on the columns. Some scholars have proposed restraining measures such as restraining casing, corner bracing, and internal straight stiffeners [1,2]. The stiffening measures for the concrete-filled steel tubular (CFST) composite columns are mainly steel casings and FRP casings. The load-bearing capacity and durability of the CFRP-wrapped CFST are improved [3,4], and measures such as stiffeners, corner braces and tie rod are mainly applied to rectangular concrete-filled steel tubular columns [5,6]. Cai et al. [7] studied the square-section concrete column with the tie rod. The results show that the restraint tie rod can effectively delay the local buckling of the steel tube and improve the bearing capacity and deformation capacity of the member. The restraining effect is affected by the strength and spacing of the tie rod. Liu and Cheng [8] studied the bearing capacity and failure mode of the concrete-filled steel tubular short columns under axial compression with open-hole steel plate. It was found that the opening stiffener can effectively improve the stability of the steel pipe wall, the failure mode of the test piece and the stiffener stiffness are highly correlated. Yang et al. [9] carried out experimental research on the concrete-filled steel tubular columns with pull-tabs and corners. The results show that the corner brace and the pull-tab can delay the local buckling of the steel pipe and improve the ductility of the components. The effects of corner bracing are better. Tong and Yu [10] carried out multi-stage loading tests on six circular steel tubular concrete axial compression short columns. The test found that the multi-stage loading of the early age round concrete-filled steel tubular columns is obvious, and the bearing capacity is less affected after 28 days of ageing. Jones and Wang [11] studied the bending and shears properties of concrete-filled steel tubular columns with inner ring plates. It was found that the strength of the inner ring-plate concrete filled with concrete was improved, especially for shear strength. In order to delay the local buckling of the thin-walled steel pipe structure, the bearing capacity of the component was improved, and the mechanical property degradation of the component in the elastoplastic phase is slowed down. Zuo et al. [12] carried out the axial compression test of T-shaped concrete-filled steel tube with restrained tie rods, and studied the axial compression performance of the tensile strength,

* Autor corespondent/*Corresponding author*,
E-mail: wangdayuwang@126.com

stiffener can effectively and bearing capacity of different tensile rod spacing, diameter and steel plate thickness. Tao et al. [13] carried out the axial compression test of 36 concrete columns with and without ribbed steel pipes, and investigated the influence of different ribbing methods, and obtained the optimal form. Manojkumar et al. [14] obtained a linear regression model for the axial compression test of 81 concrete-filled steel tubular columns. The calculation results were compared with the test and the current specifications/procedures. Liew and Xiong [15] carried out the axial compression test of 8 concrete-filled steel tubular columns. The steel pipe was pre-stressed, and then the concrete-filled steel tube section was pressed. The simulation was carried out with ABAQUS. Based on the EC4 formula, the calculation formula of steel pipe pre-pressure was proposed. Long and Cai [16] conducted a concrete axial compression test of seven restrained drawbars, and analysed the influence of the tie rods and various parameters on the columns. Chen and Sheng [17]; Ding et al. [18] carried out the axial compression test of 10 dumbbell-shaped CFST columns, studied the difference between the slenderness ratio and the instability axis, and the axial compression performance of the long column. The numerical simulation analysis was carried out with ANSYS.

However, the diameter-to-thickness ratio (width-thickness ratio) of steel pipes has a significant effect on the structural behaviour of TWCFST columns, particularly in the local buckling behaviour. Therefore, the TWCFST column with spiral stiffeners is proposed. The stiffeners are spirally distributed along the steel pipe, and the stiffness distribution is uniform, which can better restrain the local deformation of the thin-walled steel pipe. For horizontal loads, the spiral stiffeners also provide certain strength. The spiral stiffener has a built-in form; the built-in spiral stiffener can solve the problem of bond-slip of steel pipe and concrete, and enhance the overall performance of the component, in addition to restraining the steel pipe. In this paper, the axial compression test of thin-walled CFST composite columns with spiral stiffeners is carried out. The failure mode, bearing capacity and deformation capacity of the new composite members are studied, which can provide certain technical support for the engineering application of the new composite columns.

2. Experiment Programme

2.1 Details of the columns

A total of 4 different types of thin-walled concrete-filled steel tubular columns were designed and manufactured, and the cross-section of the test piece was shown in Fig.1. The specimens were divided into ordinary and stiffener pipes; the stiffeners were distributed helically along the inside of the steel tube. The design parameters of the components were shown in Table 1. The test steel pipe and stiffeners were made of Q235 grade steel, and the stiffeners were formed: firstly, the spiral stakeout (semicircle = semi-helical stiffener length) was carried out on the steel plate, and then the whole steel was stretched and formed, and finally the steel film was shaped. The properties of steel materials were shown in Table 2. In order to ensure that the steel pipe and the concrete could be stressed at the same time during the loading process, the end plate was welded at the end of the component according to the section size. And in order to facilitate the pouring of the central end plate of the concrete end plate D=160mm, the lower part of the end plate was opened with a lead groove; the width was 10 mm, and the depth was 8 mm. The steel pipe was filled with C30 self-compacting concrete, using 32.5 grade Portland cement. Coarse aggregate was continuous graded crushed stone, the particle size was 5~10 mm, the fine aggregate was medium fine sand, the mixing water was tap water, and the admixture was polycarboxylate. The mixing ratio of acid high-performance water reducing agent was shown in Table 3.

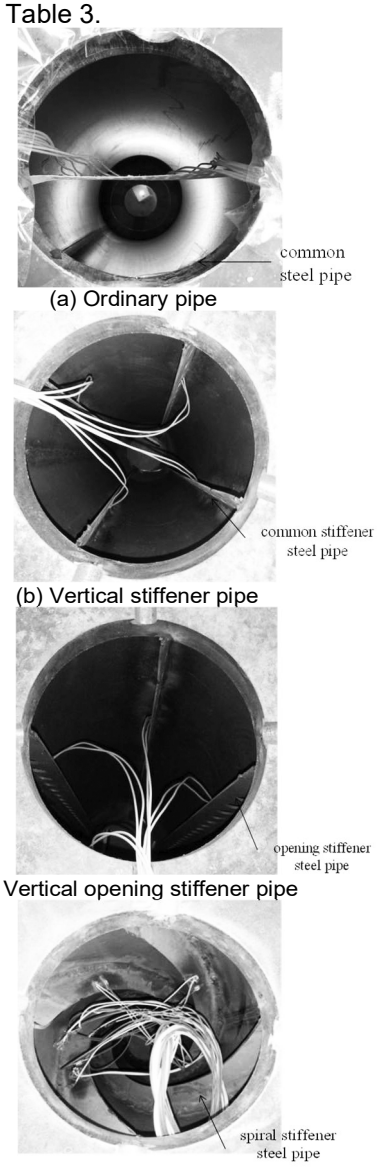

(a) Ordinary pipe

(b) Vertical stiffener pipe

(c) Vertical opening stiffener pipe

(d) Spiral stiffener pipe

Fig.1 - Section forms

Table 1

Parameters of specimens

No.	Stiffening form	Height H/mm	Outer diameter D/mm	Tube thickness t/mm	Stiffener width b_s/mm	Stiffener thick t_s/mm	Diameter to thickness ratio
Z0	--	1050	260	1.5	--	--	173
Z1	vertical stiffener	1050	260	1.5	40	3	173
Z2	vertical opening stiffener	1050	260	1.5	50	3	173
Z3	spiral stiffener	1050	260	1.5	40	3	173

Table 2

Mechanical performance indexes of steel

steel	E/MP$_a$	f_y/MP$_a$	f_u/MP$_a$	$\Delta L/L$
Steel Pipe(1.5mm)	2.01×10^5	241.94	361.85	34.06%
Steel Pipe(2mm)	2.03×10^5	253.62	379.39	30.27%
Spiral ribbed pipe(3mm)	2.06×10^5	266.43	404.35	26.54%

Note: E is the elastic modulus; f_y is the yield strength; f_u is the tensile strength; $\Delta L/L$ is the elongation.

Table 3

Mix proportion of concrete

strength grad	Cement /kg·m^{-3}	fly-ash /kg·m^{-3}	Sand /kg·m^{-3}	Rubble /kg·m^{-3}	Water /kg·m^{-3}	water-reducing admixture /kg·m^{-3}	f_{cu}/MPa	E_c/GP$_a$
C30	391.2	123.9	767	987	180	5.03	38.1	25.4

Note: f_{cu} is the compressive strength of cubic concrete test block; E_c is the concrete elastic modulus.

2.2 Loading and testing scheme

The loading device is a 5000 kN long-column pressure testing machine, and the loading device is shown in Fig.2. The loading method is a grading loading method combining load and displacement. The midpoint of the test piece is aligned with the midpoint of the upper and lower plates of the test machine by a laser line finder. Preloading is performed before the test to check the working state of the test instrument, and eliminate the internal clearance between the specimen and the loading device. The formal loading is carried out firstly using load control, and the loading rate is 1 kN/s. The loading method changes to displacement control when the load reaches 0.85 times of the estimated limit load, and the loading rate is 0.35 mm/s. And the loading is stopped when the vertical displacement of the test piece reaches 2 to 3 times of the yield displacement or the load drops to 0.75 times of the ultimate load.

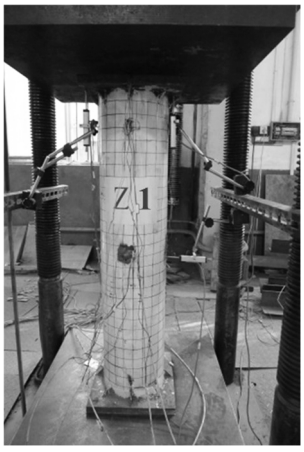

Fig.2 - Test setup

The measuring point arrangement is shown in Fig.3. The longitudinal displacement is measured by two displacement gauges arranged at the top of the test piece, and the lateral displacement is measured by a displacement meter placed in the middle of the test piece; the longitudinal strain is placed 200 cm from the top and bottom of the test piece. The longitudinal and transverse strain gauges are arranged in the middle of the test piece; longitudinal and transverse strain gauges are arranged on the 300 mm spiral stiffener from the top of the column.

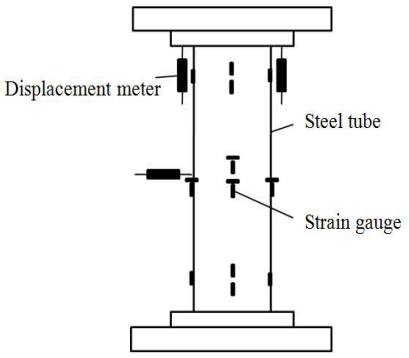

Fig.3 - Main measuring points arrangement

3. Test Phenomenon

At the initial stage of loading, the load and displacement of the specimen Z0 were linear, and the steel pipe did not change significantly. When the load increased to 1200 kN, due to the processing defects, local micro-drum appeared 80 mm from the top of the test piece, accompanied with sounds like “Papa”, and before the ultimate load, the test piece did not change significantly; when the load

increased to 1687.4 kN, the drum was obviously 50 mm and 300 mm from the top of the test piece, and the length of the drum ripple was about 1/2 of the test piece circumference, as shown in Fig.4. In order to observe the internal concrete failure mode, the steel pipe was cut after the end of the test. As can be seen from Fig.4, the concrete was crushed and broken at 300 mm from the top of the column, and a 45-degree oblique crack occurred in the concrete crushed portion.

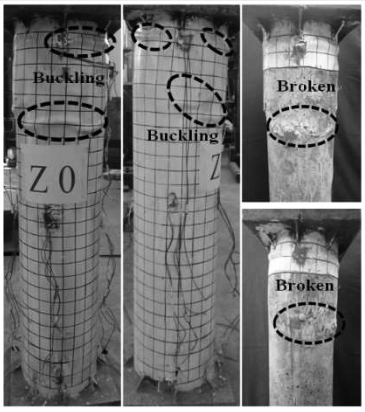

Fig.4 - Failure modes of ordinary TWCFST column

Z1 is a concrete column with vertical ribbed steel tube. The initial test piece is in the elastic stage without obvious change. When the load increased to 1400 kN, due to the processing defects, local micro-drum appeared 50 mm from the top of the test piece. When load increased to 1700 kN, the drum was bent at 250 mm from the top of the test piece and gradually formed ripples. The drum was gradually increased with the load, and then loaded. No other buckling appeared during the process. When load increased to 2010 kN, the steel plates on both sides of the stiffeners in the middle part of the test piece were slightly bulged. As the displacement increased, the drums developed, as shown in Fig.5. When the steel pipe was cut, it was found that the concrete was crushed at the drums, and the failure surface was 45 degrees.

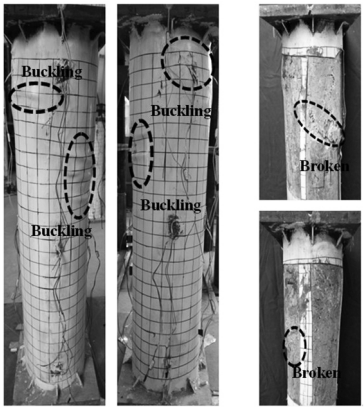

Fig.5 - Failure modes of vertical stiffener TWCFST column

Z2 is a concrete column with vertical opening ribbed steel tube. The initial test piece is stable without obvious change. When the load increased to 1915 kN, the drum was bent at 60 mm from the top of the test piece and gradually forms ripples. When the load decreased to 1800 kN, the drum occurred at 100 mm from the top of the test piece. When the load decreased to 1700 kN, the drum occurred at 150 mm from the bottom of the test piece. As the displacement increased, the drums developed, as shown in Fig.6. When the steel pipe was cut, it was found that the concrete was crushed at the drums.

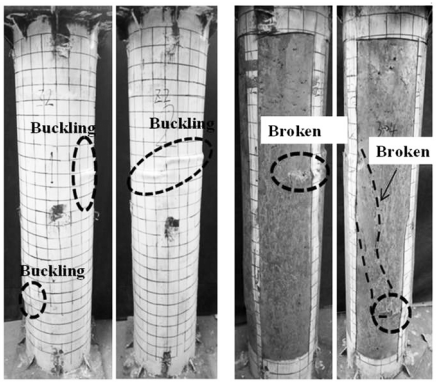

Fig.6 - Failure of vertical opening stiffener TWCFST column

Z3 is a concrete column with spiral ribbed steel tube. The initial test piece is in the elastic stage without obvious change. When load increased to 1600 kN, the drum was bent at 60 mm from the top of the test piece and gradually formed ripples. The drum was gradually increased with the load, and then loaded. No other buckling appeared during the process. When load increased to 1800 kN, the steel plates on both sides of the stiffeners in the middle part of the test piece were slightly bulged. As the displacement increased, the drums developed along the stiffeners to the ends of the test piece and spirally distributed, accompanied by paint cracking sound. After the loading, the specimen was broken like a "twist", and the drum was slightly drummed and evenly distributed, as shown in Fig.7.

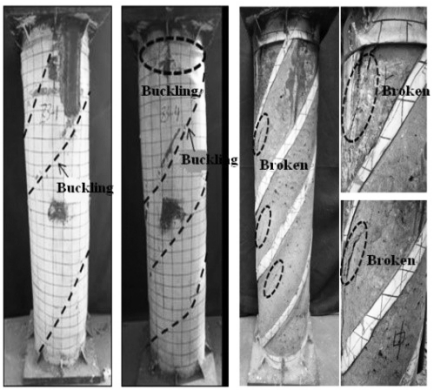

Fig.7 - Failure of spiral stiffener TWCFST column

When the steel pipe was cut, it was found that the concrete at both ends of the test piece was crushed. Except for the two ends, the rest of the concrete was uniformly drummed along the spiral stiffener. The upper part of the column showed multiple cracks along the direction of the spiral stiffener. The concrete damage was distributed in the centre of adjacent spiral stiffeners, as shown in Fig.7.

4. Analysis of Test Results

4.1 Load-displacement curve

Fig.8 shows the load-displacement curve of TWCFST columns. It can be seen from the figure that the influence of the stiffener on the bearing capacity is significant. And the bearing capacity of vertical stiffener, vertical opening stiffener and spiral stiffener of TWCFST columns are 19%, 14% and 6% higher than that of the ordinary TWCFST column, respectively. From the perspective of deformability, the stiffeners can improve the deformability of TWCFST column.

When the ultimate load is reached, the bearing capacity of Z0, Z1 and Z2 decrease to some extent as the test continues, and the bearing capacity will decrease slowly after Z1 reaches the ultimate bearing capacity. The bearing capacity of Z3 decreases slowly after the ultimate load.

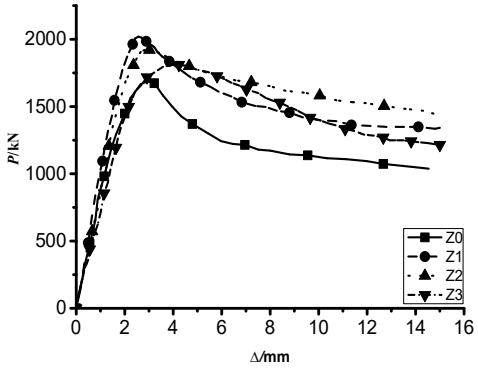

Fig.8 - Load-displacement curves

4.2 Load-strain curve

Fig.9 shows the load-strain curves for the Z0 to Z3 specimens. Compared Fig.9(a) to 9(d), it is found that the initial test pieces are in the elastic stage, and the longitudinal strain and the transverse strain of the Z0, Z1 and Z2 increase with the load. However, the longitudinal strain and transverse strain of Z3 is relatively small before reaching the ultimate bearing capacity, indicating that the built-in spiral stiffener can effectively delay the local buckling of the steel pipe. After reaching the ultimate bearing capacity, the longitudinal strain and the transverse strain increase rapidly. This is due to the combination of the internal spiral stiffener and the concrete after the internal concrete is crushed; compared with Z0, the transverse strain of Z1 and Z2 are significantly reduced when the specimen is broken, but the transverse strain of Z3 is not significantly reduced. This shows that the spiral stiffener and concrete can be better combined after concrete crushing, which effectively limits the lateral deformation of the steel pipe.

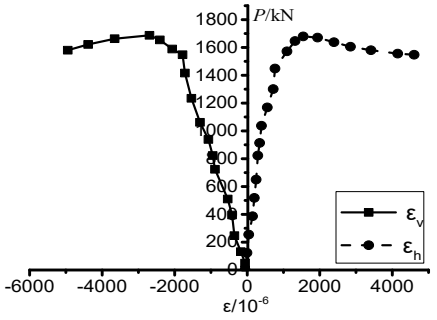

(a) Z0

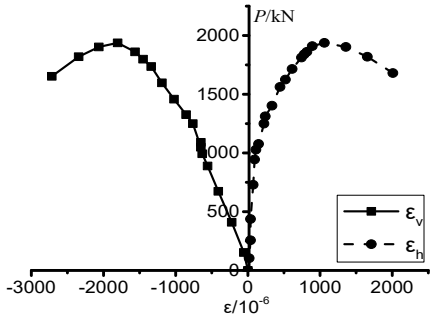

(b) Z1

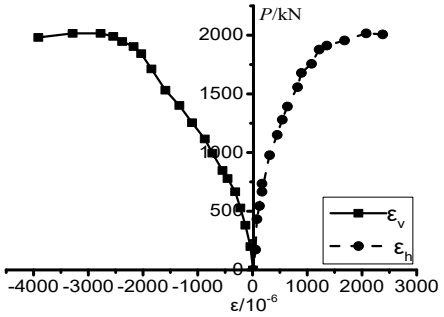

(c) Z2

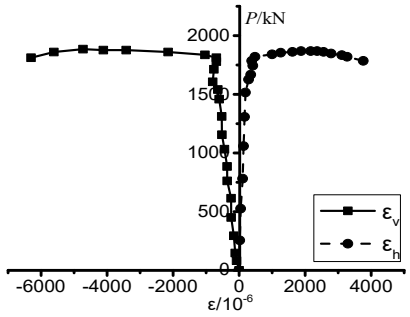

(d) Z3

Fig.9 - Load-strain curves

4.3 Transverse deformation coefficient

The stress state of the specimen under axial load is analyzed by the relationship between the load and the transverse deformation coefficient *U* ($U = \left|\frac{\varepsilon_h}{\varepsilon_v}\right|$). It can be seen from Fig.10 that the transverse deformation coefficient roughly conforms to Z3<Z1<Z0<Z2 before the load reaches 80% of the peak load, indicating that the built-in stiffeners can effectively limit the lateral deformation of the test piece. When the load reached the ultimate load, the lateral deformation coefficient changed sharply, but the difference between the 4 test pieces was not large, as show in Fig.10.

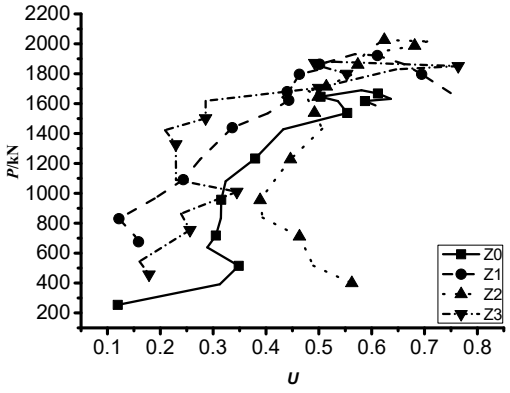

Fig.10 - Lateral deformation coefficient

4.4 Failure mode and mechanism

As shown in Fig.11, Z3 is distributed around the wall of the steel pipe due to the inner spiral stiffener. After the failure, the top of the test piece shows a ring-shaped bulge, and the wall of the steel pipe has a spiral-shaped bulge like a “fried dough twist” shape, and the spiral stiffener is combined with the concrete. The deformation of the steel pipe wall has a certain limiting effect in the longitudinal and lateral directions. After the inner spiral stiffener is set, the drum wall of the steel pipe is obviously smaller and the drum bending distribution is more uniform. The concrete inside the column top is crushed, and the concrete drum outside the column is spiral, and the crack is confined to the adjacent two spiral stiffeners.

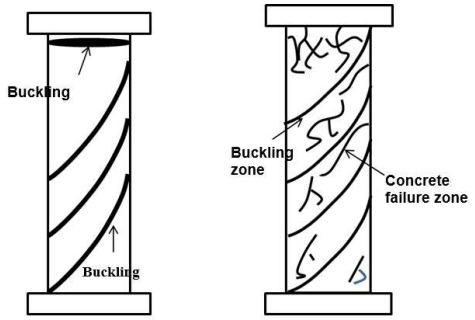

Fig.11 - Failure mode

Under vertical load, the concrete undergoes vertical and lateral deformation. The steel tube is restrained by the spiral ribs, the lateral deformation is reduced. The internal concrete is restrained and the bearing capacity is increased, the external concrete is also subjected to less lateral compression, the stress variation is more favorable.

5. Finite Element Calculation

5.1 Transverse deformation coefficient

The finite element simulations of the test components Z0 and Z1 were carried out by ABAQUS software, and compared with the experimental data, the strength criterion selected by the finite element analysis and the rationality of the constitutive relation were verified, and the basis for the parameter analysis of the components was provided. According to the results of the material test, the steel pipe: $E=2.01\times10^5$ MP_a, the yield strength $f_y=242$ N/mm^2, the tensile strength $f_u=362$ N/mm^2; the stiffener: $E=2.06\times10^5$ MP_a, the yield strength $f_y=266$ N/mm^2, the tensile strength $f_u=404$ N/mm^2; concrete: $E_c=25.4$ GP_a, the compressive strength $f_c=28.9$ N/mm^2. The concrete adopted the plastic damage model and the yield criterion. The constitutive relationship of steel was a bilinear isotropic strengthening model with a yield criterion of Von Mises. The steel tube and stiffeners used a four-node reduced integral shell element (S4R), and the Simpson integral of 9 integral points was used in the thickness direction to meet the calculation accuracy requirements. The three-bit solid unit of the 8-node reduction integral was selected for the loading end plate and concrete. Steel pipe, stiffeners and concrete were selected from the Sweep division technique and the neutral axis algorithm (Medial Axis). The loading end plate used the Structured Grid division technique and the Medial Axis algorithm. A schematic diagram of the meshing of the finite element model of a thin-walled concrete-filled steel tubular column was shown in Fig.12. The interface relationship between steel pipe and concrete was defined as face contact, steel pipe and stiffener were defined as binding constraints and the constraint relationship between end plate and stiffener and steel pipe was defined as shell-solid coupling constraint, and the end plate was bonded and connected with concrete.

The failure modes of the specimens Z0 and Z3 and the deformation cloud diagram of the concrete in the steel pipe and the pipe wall calculated by the finite element were shown in Fig.13. The steel pipe wall was outwardly bulged or locally buckling; the deformation of the test piece could be seen from the deformation cloud diagram that there was a great relationship between the deformation of the specimen and the form of stiffener. Due to the relatively small stiffness of the Z0 test piece, the finite element calculation first occurred in the upper part of the pipe wall, which was consistent with the

test phenomenon. For the test piece Z3, the stiffened stiffeners began to buckle after the yielding of the stiffened stiffener, effectively delaying the steel pipe wall. The local buckling was consistent with the experimental failure mode. But the fracture morphology of the specimen Z0 was expressed as the middle and upper drum, which is different from the central drum of the finite element calculation result, due to the quality of welding, concrete pouring and so on. The final failure mode of the specimen Z3 test and the calculated deformation cloud map were well fitted.

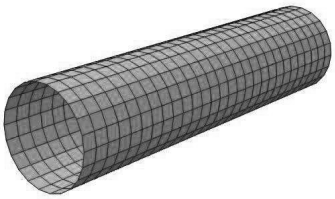

(a) Steel Pipe

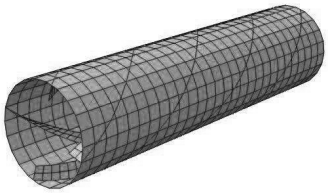

(b) Spiral stiffener steel pipe

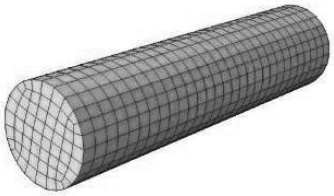

(c) Concrete

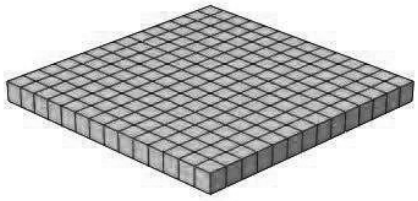

(d) End plate

Fig.12 - Schematic diagram of the meshes of specimen

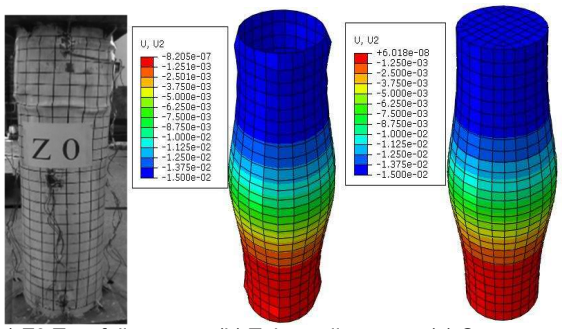

(a) Z0 Test failure form (b) Tube wall deformation cloud (c) Concrete deformation cloud

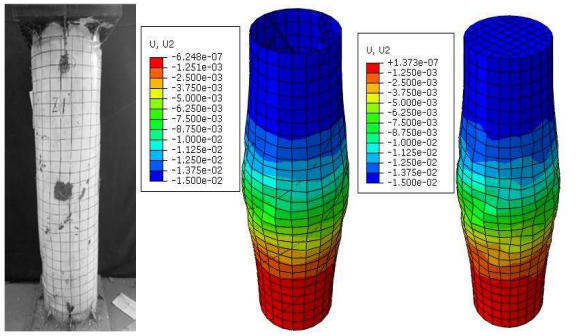

(d) Z3 Test failure form (e) Tube wall deformation cloud (f) Concrete deformation cloud

Fig.13 - Comparison of damage patterns of specimens

5.2 Parameter analysis

5.2.1 Parameter setting

The finite element software was used to analyse the parameters of the spiral-shaped thin-walled concrete-filled steel tubular columns. The diameter-thickness ratio of the circular steel tube, the width-thickness ratio of the spiral stiffeners and the influence of the pitch on the mechanical properties were studied. The specific parameters were shown in Table 4. The steels of all specimens were Q235 and the concrete strength was C30, and the parameters were the parameters used in the finite element model of the previous chapter.

Table 4

List of specimen parameters

No.	Test piece number	*D*/mm	*t*/mm	*L*/mm	*D/t*	$b_s \times t_s$	b_s/t_s	Pitch *R*/mm
1	Z260a	260	1.5	1050	173.3	40×3	13.3	1050
2	Z260b	260	2.0	1050	130	40×3	13.3	1050
3	Z260c	260	2.5	1050	104	40×3	13.3	1050
4	Z260d	260	3.0	1050	86.7	40×3	13.3	1050
5	Z260-1a	260	1.5	1050	173.3	30×3	10	1050
6	Z260-2a	260	1.5	1050	173.3	50×3	16.7	1050
7	Z260-3a	260	1.5	1050	173.3	30×2	15	1050
8	Z260-4a	260	1.5	1050	173.3	40×2	20	1050
9	Z260-5a	260	1.5	1050	173.3	50×2	25	1050
10	Z260-2b	260	2.0	1050	130	40×3	13.3	1575
11	Z260-1b	260	2.0	1050	130	40×3	13.3	525

Note: In the above table, *D* is the diameter of the test piece, *t* is the thickness of the round steel pipe, *L* is the length of the test piece, b_s and t_s are the width and thickness of the stiffener, respectively, and *D/t* is the ratio of the diameter to the thickness of the test piece, b_s/T_s is the aspect ratio of the stiffener.

5.2.2 Stress cloud

Fig.14 to Figure 16 respectively show the axial stress cloud diagrams of concrete-filled steel tubes with different steel tube thickness, different pitches and different stiffener widths and thicknesses.

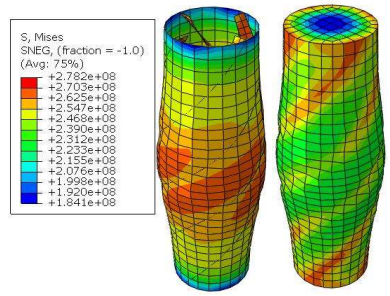

(a) Z260a(t=1.5mm)

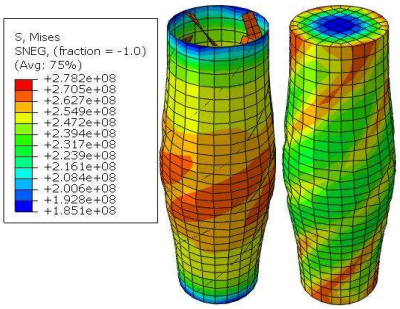

(b) Z260b(t=2mm)

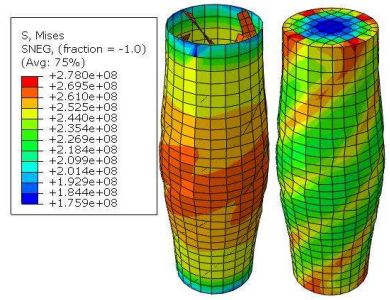

(c) Z260c(t=2.5mm)

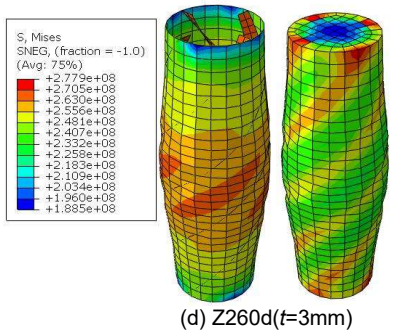

(d) Z260d(t=3mm)

Fig.14 - Comparison of stress curves of concrete-filled steel tubes with different thicknesses

From the comparison of the stress-cement diagrams of the concrete-filled steel tubes with different steel tube thicknesses in Fig.14, it can be found that the stress values of the steel pipe walls are not much different when the test pieces are loaded to the end, but the stress distribution is more uniform with the increase of the thickness of the steel pipes, and the concrete is at both ends. The stress distribution around the stiffener is concentrated, and the overall stress distribution tends to be uniform with the increase of the thickness of the steel tube.

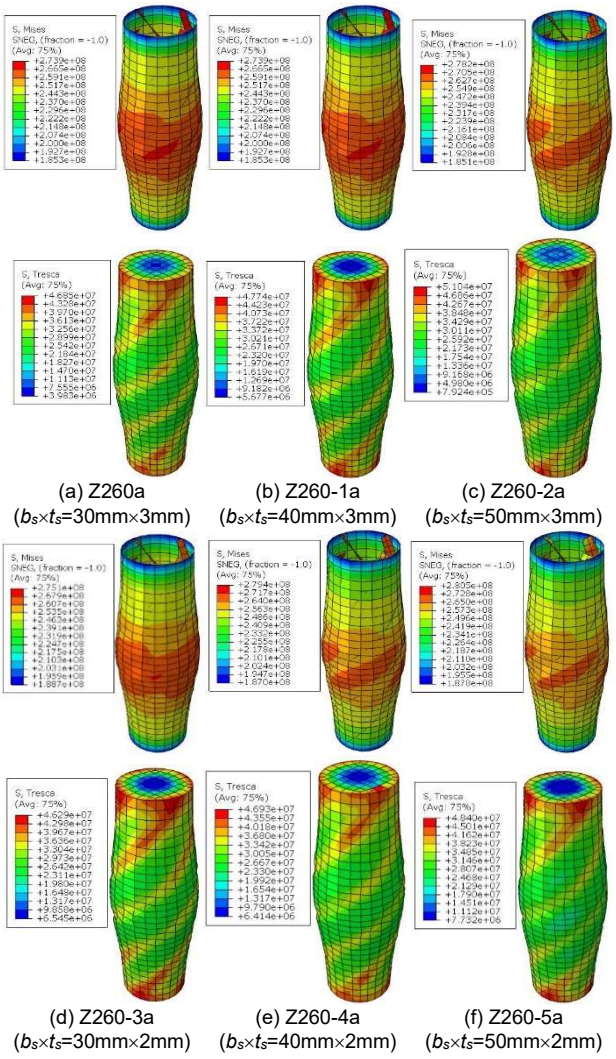

(a) Z260a (b_s×t_s=30mm×3mm) (b) Z260-1a (b_s×t_s=40mm×3mm) (c) Z260-2a (b_s×t_s=50mm×3mm)

(d) Z260-3a (b_s×t_s=30mm×2mm) (e) Z260-4a (b_s×t_s=40mm×2mm) (f) Z260-5a (b_s×t_s=50mm×2mm)

Fig.15 - Comparison of compressive stress curves of concrete-filled steel tube with different stiffener width

From the axial compression stress cloud diagram of the concrete-filled steel tube with different stiffener widths in Fig.15, it can be found that the stress on the steel pipe and the concrete increases with the increase of the width of the stiffener regardless of the thickness of the steel pipe wall of 2 mm or 3 mm, and the stress concentration on the concrete also increases with the width of the stiffener, and the stress distribution tends to be uniform.

From the axial stress cloud diagram of concrete-filled steel tube with different pitches in Fig.16, it can be found that the smaller the pitch of the spiral stiffener, that is, the smaller the distance between the stiffeners, the stronger the restraining effect of the steel tube on the concrete, and the more uniform the stress distribution on the concrete.

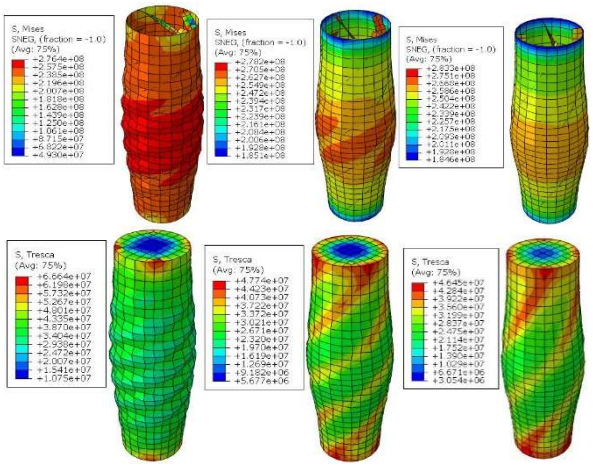

(a) Z260-1b (R=525mm) (b) Z260b (R=1050mm) (c) Z260-2b (R=1575mm)

Fig.16 -Comparison of axial compressive stress of con crete-filled steel tube with different pitch

6. Analysis of Factors Affecting Mechanical Properties

6.1 Steel pipe diameter to thickness ratio D/t

Fig.17 shows the load-displacement curves of various types of test pieces. It can be seen from the figure that the load-displacement curves of each test piece have different degrees of descending after the peak value, and with the increase of the diameter-thickness ratio D/t of the steel pipe, the trend of decline is more and more obvious, and the ductility also has a certain degree of decline.

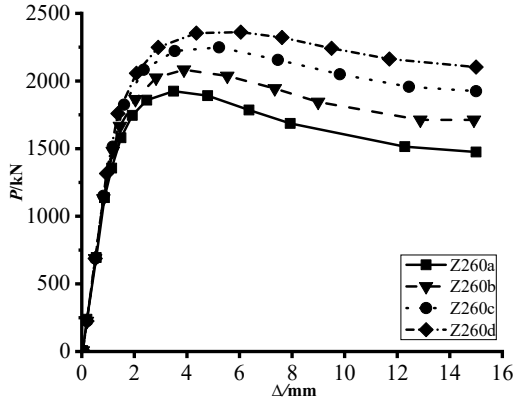

Fig.17 - Curves contrast for steel pipe diameter to thickness ratio

6.2 Stiffener width ratio

It can be seen from Fig.18 to 19 that under the same conditions, the influence of the width and thickness of the stiffener on the stress distribution on the steel pipe and concrete is not obvious. The general rule is that with the increase of the width and thickness of the stiffener, the steel pipe and the stress distribution on concrete tend to be evenly distributed.

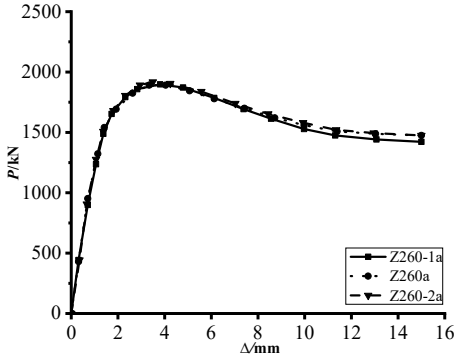

Fig.18 - Curves contrast for stiffener 3 mm width

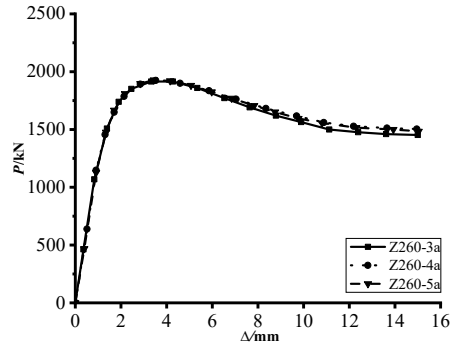

Fig.19 - Curves contrast for stiffener 2 mm width

6.3 Pitch

Through calculation and analysis, it can be found that the influence of stiffener width and thickness on the mechanical properties of concrete-filled steel tubular columns is very small. Therefore, in this paper, specimens with a diameter of 260 mm, a thickness of 2 mm, a width of 40 mm and a thickness of 3 mm were selected to analyse the influence of pitch on the mechanical properties of concrete-filled steel tube columns. Fig.20 shows the steel pipe with stiffener spacing of 525 mm, 1050 mm and 1575 mm. It can be seen that the load-displacement curve of the concrete-filled steel tubular column with a pitch of 525 mm is very gentle in the falling section after the peak crossing. And it shows good ductility, compared with concrete filled steel tube columns with pitch of 1050mm and 1575mm, but the variation of the stiffener spacing has little effect on the ultimate bearing.

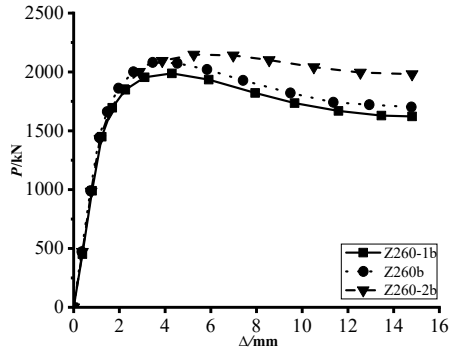

Fig.20 - Curves contrast for pitch

7. Conclusion

(1) Under the axial compression load, the ordinary TWCFST short column has many local buckling parts and the buckling is serious. The internal concrete is a shear fracture and the crushing range is large. The built-in stiffeners can effectively delay the local buckling of the steel pipe wall. The local buckling is evenly distributed along the pipe wall, and the internal concrete failure interface is evenly distributed along the column.

(2) The internal spiral stiffener can improve the axial bearing capacity of the concrete-filled steel tubular column, which is 6% higher than that of the ordinary concrete-filled steel tubular column; after reaching the ultimate bearing capacity, the bearing capacity of the inner spiral stiffener specimen is reduced with the increase of the displacement slow.

(3) Compared with the ordinary steel tube concrete, after the inner spiral stiffener is set, the spiral stiffener is tightly combined with the concrete; the confinement effect of the spiral stiffener is evenly distributed, and the deformation of the steel tube and the stiffener is more coordinated.

(4) When the thickness of the thin-walled steel pipe, the width and thickness of the stiffener, and the pitch are constant, the stress distribution on the steel pipe increases with the increase of the diameter-to-thickness ratio D/t of the steel pipe, and the ductility is more and more obvious. There is a certain degree of decline. Under the same conditions, with the increase of the width and thickness of the stiffener, the stress distribution on the steel pipe and concrete tends to be evenly distributed.

(5) The variation of the spiral stiffener spacing has a great influence on the ductility of the test piece. The load-displacement curve of the concrete-filled steel tubular column with a pitch of 525 mm is very gentle in the descending section after the peak crossing, compared with the concrete-filled steel tubular column with the pitch of 1050 mm and 1575 mm. It shows good ductility, but the change in stiffener spacing has little effect on the ultimate load.

Acknowledgments

The authors gratefully acknowledge financial support from the National Natural Science Foundation of China (Grant No. 51668053), Scientific research project of Xi'an University of Technology (2015CX016), Construction science and technology project of the ministry of housing and urban-rural construction in Shaanxi province (2016-K91), Basic research program of natural science in Shaanxi province (Young talent project) (2017JQ5032), Projects funded by the China Postdoctoral Science Fund (2017M613174), Shaanxi association for science and technology of universities young talent support project (20170513).

REFERENCES

[1] C. Petrus, H.A. Hamid, A. Ibrahim, G. Parke, Experimental behavior of concrete filled thin walled steel tubes with tab stiffeners. Journal of Constructional Steel Research, 2010, **66**(7), 915-922.

[2] Z. Tao, Development status of concrete filled steel tube structure. Building Structure, 2003,**33**(07), 20-23+35.

[3] S. Li. Y.Y. Lu, Experimental study on shear resistance performance of concrete filled circular FRP-steel tube columns. Journal of Building Structures, 2012,**33**(11), 107-114.

[4] M.X. Liu, J.R. Qian, Moment-curvature relationships of FRP-concrete-steel double-skin tubular members. Journal of Tsinghua University(Science and Technology), 2007, **37**(12), 2105-2110.

[5] C.X. Xu, C.A. Zhu, Experimental research on concrete-filled square thin-walled Steel tubular stub columns with steel bar stiffeners. Journal of Building Structures, 2009, **30**(S2), 231-236.

[6] N. Sotehi, I. Tabet, A. Chaker, Combined experimental and numerical characterization of thermal properties of lightweight concretes used in construction. Annales de Chimie - Science des Matériaux, 2018, **42**(2), 245-258.

[7] J. Cai, X.Z. Zheng, Q.J.Chen, Z.L.Zuo, Experimental study on axial compression behavior of stiffened square section CFST short columns. Journal of Building Structures, 2014, **35**(3), 178-185.

[8]Y.J.Liu, G. Cheng, Experimental research on concrete-filled square steel tubular columns stiffened with PBL. Journal of Building Structures, 2014, **35**(10): 39-46.

[9]Y.L. Yang, Y.Y. Wang, Feng Fu, Effect of reinforcement stiffeners on square concrete-filled steel tubular columns subjected to axial compressive load. Thin-Walled Structures, 2014, **82**(9), 132-144.

[10] D.H. Tong, M.Yu, Experimental research on influence of multi-level loading on axial compression behavior of concrete-filled circular steel tubular short columns. Journal of Building Structures, 2017,**38**(S1), 241-248.

[11] M.H. Jones, Y.C. Wang, Shear and bending behaviour of fin plate connection to concrete filled rectangular steel tubular column-development of a simplified calculation method. Journal of Constructional Steel Research, 2011, **67**(3), 348-359.

[12] Z.L. Zuo, J. Cai, M.F. Liu, W.N. Duan, Q.Q. Chen, Experimental study on T-shaped CFST stub columns with binding bars subjected to axial compression. China Civil Engineering Journal, 2011, **44**(11), 43-51.

[13] Z. Tao, L.H. Han, D.Y. Wang, Strength and ductility of stiffened thin-walled hollow steel structural stub columns filled with concrete. Thin Walled Structures, 2008, **46**(10), 1113-1128.

[14] M.V. Chitawadagi, M.C. Narasimhan, S.M. Kulkami, Axial capacity of rectangular concrete-filled steel tube columns-DOE approach. Construction and Building Materials, 2010, **24**(4), 585-595.

[15] J.Y.R. Liew, D.X. Xiong, Effect of preload on the axial capacity of concrete-filled composite columns. Journal of Constructional Steel Research, 2009, **65**(3), 709-722.

[16] Y.L. Long, J. Cai, Experimental Investigation into Axial Compressive Behavior of L-Shaped Concrete-Filled Steel Tubular Stub Columns with Binding Bars. Journal of South China University of Technology(Natural Science Edition), 2006, **34**(1), 87-92.

[17] B.C. Chen, Y. Sheng, Research on Load-Carrying Capacity of Concrete-Filled-Steel Tubular Dumbbell-Shsped Long Colomns Under Axial Loads. Engineering Mechanics, 2008, **25**(4), 121-133.

[18] F.X. Ding, D.R. Lu, Y. Bai, Q.S. Zhou, Comparative study of square stirrup-confined concrete-filled steel tubular stub columns under axial loading. Thin-Walled Structures, 2016, **98**(1), 443-453.

****